Structural Engineering and Mechanics, *Vol. 56, No. 2 (2015) 275-291*
DOI: http://dx.doi.org/10.12989/sem.2015.56.2.275

Investigation of bond-slip modeling methods used in FE analysis of RC members

Serhat Demir* and Metin Husem[a]

Department of Civil Engineering, Karadeniz Technical University, 61080, Trabzon, Turkey

(Received January 28, 2015, Revised August 16, 2015, Accepted October 19, 2015)

Abstract. Adherence between reinforcement and the surrounding concrete is usually ignored in finite element analysis (FEA) of reinforced concrete (RC) members. However, load transition between the reinforcement and surrounding concrete effects RC members' behavior a great deal. In this study, the effects of bond-slip on the FEA of RC members are examined. In the analyses, three types of bond-slip modeling methods (perfect bond, contact elements and spring elements) and three types of reinforcement modeling methods (smeared, one dimensional line and three dimensional solid elements) were used. Bond-slip behavior between the reinforcement and surrounding concrete was simulated with cohesive zone materials (CZM) for the first time. The bond-slip relationship was identified experimentally using a beam bending test as suggested by RILEM. The results obtained from FEA were compared with the results of four RC beams that were tested experimentally. Results showed that, in FE analyses, because of the perfect bond occurrence between the reinforcement and surrounding concrete, unrealistic strains occurred in the longitudinal reinforcement. This situation greatly affected the load deflection relationship because the longitudinal reinforcements dominated the failure mode. In addition to the spring elements, the combination of a bonded contact option with CZM also gave closer results to the experimental models. However, modeling of the bond-slip relationship with a contact element was quite difficult and time consuming. Therefore bond-slip modeling is more suitable with spring elements.

Keywords: stress transfer; bond-slip; finite element analysis; reinforced concrete beam; ANSYS

1. Introduction

Experimental studies are extremely important in civil engineering. These studies have the lead role in regards to the continuing development of the numerical approach as well as being an irreplaceable resource for computer programs. As experimental studies can be tiring and expensive the ability to use computer programs based on the finite element method (FEM) are often utilized.

Bond-slip is one of the most significant factors to affect the behavior of RC members (Zhao and Sritharantharan 2007, Fallah *et al*. 2013). The behavior of RC members is based on the composite action between the concrete and reinforcement. In order to maintain composite action, some stress transformation between the concrete and reinforcement, known as a bond, is

*Corresponding author, Ph.D. Candidate, E-mail: s.demir@ktu.edu.tr
[a]Professor, E-mail: mhusem@ktu.edu.tr

http://www.techno-press.org/?journal=sem&subpage=8 ISSN: 1225-4568 (Print), 1598-6217 (Online)

necessary. Bond stress is best realized as a continuous stress field that develops between the steel-concrete interface. When reinforced concrete members undergo loading a relative displacement can occur between the reinforcement and surrounding concrete interface, known as bond-slip (Tepfers 1973). According to the analyses of RC members, the bond-slip relationship should be considered in modeling. Omitting the bond-slip relationship in FEA can lead to critical miscalculations in load-deflection response, stress, and strain distribution (Yang and Chen 2005, Chen *et al*. 2012, Aslani and Samali 2013, Fallah *et al*. 2013).

A bond-slip relationship can be obtained experimentally or theoretically. So far, researchers have used several experimental methods to do so, including direct pull-out, beam anchorage and beam-column joint tests, which are used in order to define adherence (Alavi and Marzouk 2002, Desnerck *et al*. 2010, Ashtiani *et al*. 2013, Kamal *et al*. 2013, Arslan and Durmuş 2014). The direct pull out test is the most commonly employed because of its easy use (Alavi and Marzouk 2002, Campione *et al*. 2005, Fang *et al*. 2006, Cattaneo and Rosati 2009). This method, however, cannot replicate the exact behavior of members under the effects of bending (Nielsen 1998, Ersoy 2012). This is because there is no vertical shear force on reinforcement and therefore local compressive stress applied to the concrete by support is too high, the concrete's cover is far too thick and there are no tension cracks in the concrete. In beams affected by bending, stress, in regards to reinforcement, increases or decreases in parallel with moment change as a direct result of adherence (Ersoy 2012). Therefore, in order to define adherence, using a beam bending test is more appropriate (Almeida *et al*. 2008, Ashtiani *et al*. 2013). Up to now, some experimental studies have been done and researchers have developed theoretical formulas giving bond-slip relationship (Mirza and Houde 1979, Eligehausen *et al*. 1983, Alfano and Crisfield 2001, Zhao and Sritharantharan 2007, Aslani and Samali 2013). These developed formulas are often used in the analyses of RC members.

In the analyses of RC members, FEM is commonly used. Although computer programs can handle numerical algorithms and material models easily, the ability to represent the actual behavior of reinforced concrete for finite element models depends on the modeling method and the accurate selection of material constitutive models (Kwan and Billington 2001, Demir *et al*. 2014). Because of the difficulty of including bond-slip relationships in the finite elements model researchers usually assume that there is full adherence (perfect bond) between the reinforcement and surrounding concrete. However, this assumption can only be valid for areas that have low stress transition. Moreover, in areas where greater stress is found, resulting in cracks, the reinforcement and concrete used will experience strain differently when bond-slip occurs. When we examine previous studies that have employed full adherence, results show that a larger load carrying capacity is achieved and more rigid behavior apparent (Yang and Chen 2005, Chen *et al*. 2012, Aslani and Samali 2013).

The most commonly used finite element software in the analyses of RC members is ANSYS (2014). This program, having the ability to simulate the debonding, cracking and crushing of concrete, enables researchers to predict the damage that can occur without performing experiments. Using numerical studies, researchers have examined the effects that different material models and reinforcements have when it comes to potential damage (Padmarajaiah and Ramaswamy 2002, Barbosa and Riberio 1998, Xiaroran and Yuanfeng 2010, Wei-ping 2011, Hawileh 2012, Altun and Birdal 2012, Marzec *et al*. 2013, Demir *et al*. 2014, Livaoglu and Durmus 2015). Commonly, however, findings on the adherence between reinforcement and the surrounding concrete are usually neglected (Barbosa and Riberio 1998, Xiaroran and Yuanfeng 2010, Wei-ping 2011, Altun and Birdal 2012). Of course, some researchers have undertaken

studies using different bond-slip models that allows for the consideration of adherence (Padmarajaiah and Ramaswamy 2002, Wei-ping 2011, Hawileh 2012, Marzec *et al*. 2013). In this study, modeling methods, which were used in the analyses of RC members, were compared. In the FEA, three different reinforcement-modeling methods and three different bond-slip modeling methods were used. The results of the FE analyses were compared with four RC beams tested experimentally.

2. Experimental study

2.1 Material properties

For the production of RC beams, CEM II/A-P 32.5 N type, cement and limestone aggregates with a maximum size of 12 mm were used. The physical properties of aggregates are given in Table 1. In each batch, 3 standard concrete cylinders (with a diameter of 150 mm and a height of 300 mm) were cast and tested to achieve the specified 28-day strength. The two end surfaces of the concrete cylinders were ground flat before compressive tests took place. Table 2 summarizes the details of the proportions mixed as well as the measurements of the material properties of the concrete. In the production of RC beams, deformed reinforcements were used. Three coupons were tested for each of the reinforcements. The properties of the reinforcements are given in Table 3.

2.2 Beam details and test setup

The experimental program consists of 4 RC beams, respectively referred to as SP1, SP2, SP3 and SP4, and all having the same properties with a cross section of 150 mm×300 mm and 2000 mm length (Fig. 1). The test set-up was designed to subject the simply supported beams to

Table 1 The physical properties of limestone aggregate

Aggregate size	Loose density (kg/m^3)	Dry density (kg/m^3)	Saturated density (kg/m^3)	Water absorption %
Course (4>mm)	1445	2706	2720	0.43
Fine (4<mm)	1485	2675	2682	0.50

Table 2 Details of the mixed proportions and measured material properties

Concrete	W/C	Cement(kg/m^3)	Water (kg/m^3)	Coarse Aggregate (kg/m^3)	Fine aggregate (kg/m^3)	Average cylinder Strength, f_c (MPa)
OC	0.50	362	181	1012	742	23.1

OC, ordinary concrete; W/C, water to cement ratio.

Table 3 Characterization of reinforcing bars

ø (mm)	α (^{o})	h_R, mm (%ø)	S_R, mm (%ø)	f_R	σ_y
8	46	1.0 (13%ø)	5 (63%ø)	0.071	496.2
12	46	1.4 (12%ø)	7 (58%ø)	0.082	517.7

ø, diameter; α, rib face inclination; h_R, rib height; S_R, rib width; f_R, relative rib area; σ_y, yielding strength

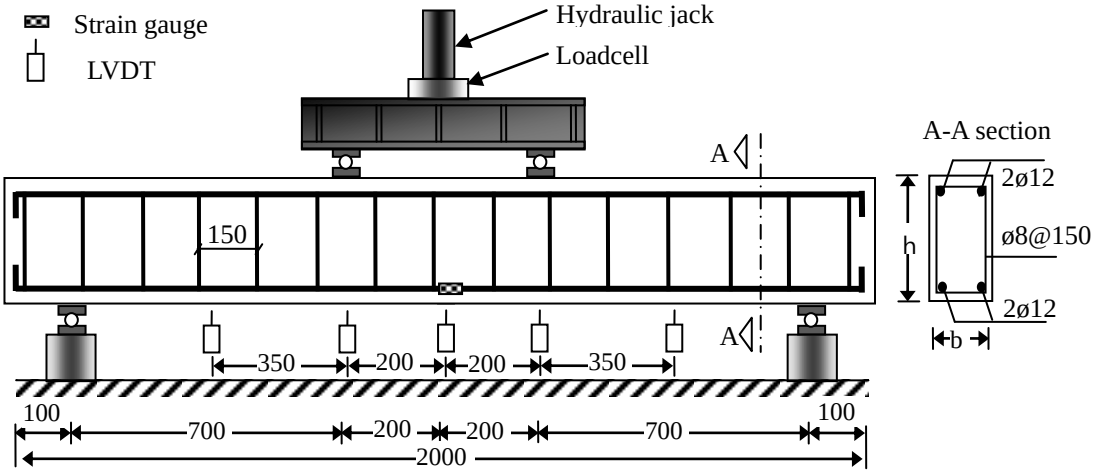

Fig. 1 Beam details and test setup

concentrated symmetrical four-point loading. Fig. 1 shows the test setup and reinforcement arrangements of the beams. Test specimens were loaded with a displacement controlled hydraulic jack. Loads were measured using a loadcell attached to the edge of a hydraulic jack and displacements were measured using LVDTs, located on the beam space. As shown in Fig. l, strains found in the longitudinal reinforcement, during the experiments, were measured using a strain gauge.

2.3 Investigation of bond-slip relations

A bond-slip relation between the reinforcement and surrounding concrete was investigated according to RILEM-FIB-CEB (1973). A total of 6 test specimens (3 for ø8 and 3 for ø12) were produced (Fig. 2(a)) and average bond-slip curves for each of the reinforcements were used in the numerical studies. The dimensions of the test specimens as well as the experimental setup recommended by RILEM, for the beam bending test, can be seen in Fig. 2(b). Test specimens consisted of two half-beams connected to each other with a steel hinge at the top-center and a deformed reinforcement at the bottom. Steel hinges were used to eliminate the compression zone of concrete in the beam under the effects of bending. The reinforcement, whose adherence is subsequently measured, is placed in the lower surface of the beam. Limitations were applied to the bond length between the reinforcement and surrounding concrete by using plastic caps at both ends of the beam at 10 times the diameter of the reinforcement (10ø). The reinforcement used was long in order to have both ends free. Subsequently, the slip in the reinforcement was measured using 0.001 mm sensitivity LVDT, which were located on both ends of the beam (Fig. 2(b)).

$$T = (P.a)/(2.h) \tag{1}$$

$$A_s = (\pi.\phi^2/4) \tag{2}$$

$$\sum(\tau_b.A_u) = T, \qquad \tau_b.(\pi.\phi).l_b = A_s.\sigma_s = \frac{\pi.\phi^2}{4}.\sigma_s \tag{3}$$

(a)

(b)

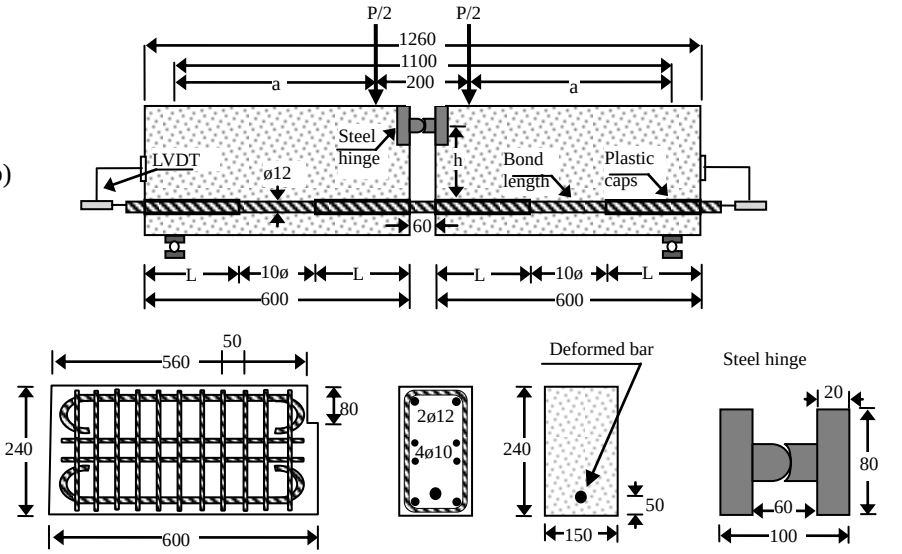

Fig. 2 (a) Test specimens, (b) Details of the beam bending test according to RILEM

$$\tau_b = (\sigma_s.\phi)/(4.l_b) \tag{4}$$

The bond stress corresponding to the tensile force, caused by the vertical load (P), was considered to have dispersed uniformly on the reinforcement. With the steel hinge having a zero moment, the tensile force (T) observed in the reinforcement, can be calculated with Eq. (1) where a is the distance between the loading point and the support and h is the moment arm. Along the bond length, the T tensile force, which effects the reinforcement in balance situations should be equal to the total adherence force, which occurs around the reinforcement. Bond stress, $\tau_{b,}$ can be measured using Eqs. (1)-(2)-(3)-(4) where A_s, A_u, ϕ, σ_s, l_b correspond to the reinforcement cross sectional area, unit area, reinforcement diameter, reinforcement stress and bond length, respectively:

3. Numerical study

Analyses of experimentally tested RC beams were conducted using ANSYS finite element software. In the analyses three different reinforcement modeling methods and three different bond-slip modeling methods were used and five different numerical models were formed.

3.1 Material properties

Material properties were defined by element type, material model and key options. Material models were defined with linear and nonlinear properties. Stress-strain relationship, modulus of elasticity, E, and poisson ratio, $\mathbf{v}$, for all elements, were defined according to experimental results. Eight node solid brick elements, Solid65, were used for the three-dimensional modeling of concrete, which can crack during tension and crush in compression, plastic deformation, and creep. Additionally, having three degrees of freedom at each node is represented via transition in the nodal and according to the x, y and z directions. A stress-strain diagram of concrete obtained experimentally was formed using multi-linear isotropic hardening plasticity (Miso) along with the Von Mises yielding criteria (Fig. 3(a)). The nonlinear behavior of concrete was modeled with the Concrete (Conc) model. This model is used to simulate failure in brittle material and it is based on William Warnke's (1974) failure criteria. Failure surface can be defined using uniaxial tensile strength, $f_{t,}$ and uniaxial crushing strength, $f_{c,}$ values. In the analyses, uniaxial tensile strength of concrete was taken 1.7 MPa. Uniaxial crushing strength can cause convergence mistakes so with this in mind -1 was applied and omitted (Kachlakev and Miller 2001, Wolanski 2004). Two other important parameters to determine the nonlinear behaviors of concrete are the shear transfer coefficients for open, β_t, and closed, β_c, cracks. Both coefficients have values between 0 and 1. These coefficients were identified as being 0.3 and 0.7, respectively (Kachlakev and Miller 2001). Stress-strain diagrams of the reinforcements obtained experimentally were formed using the bilinear kinematical hardening plasticity (Bkin) model, which is based on Von Mises yielding criteria (Fig. 3(b)).

3.2 Reinforcement modeling

Three different methods were used to model reinforcements. Firstly, smeared reinforcement was employed. In this method, the reinforcement, inside of the Solid65 element, is paramount to volumetric ratio. In the second modeling method, the reinforcement was modeled with one-dimensional line elements (Link180) and 2 nodes. In the third model, the reinforcement was modeled with three-dimensional solid elements (Solid45) and 8 nodes.

3.3 Bond-slip models

Three different bond-slip modeling methods were used in the numerical models. The first method utilized, the full adherence (perfect bond) method, is most often discussed in the literature because of the ease of use. For this method, the full adherence that occurs between the concrete and reinforcement is taken into consideration. This is why nodes, belonging to the concrete and reinforcement, were combined, therefore forming a common rigidity matrix. In the second method, the bond-slip relationship between the concrete and reinforcement nodes was modeled using spring elements (Combin39). The behavior of spring members was determined based on

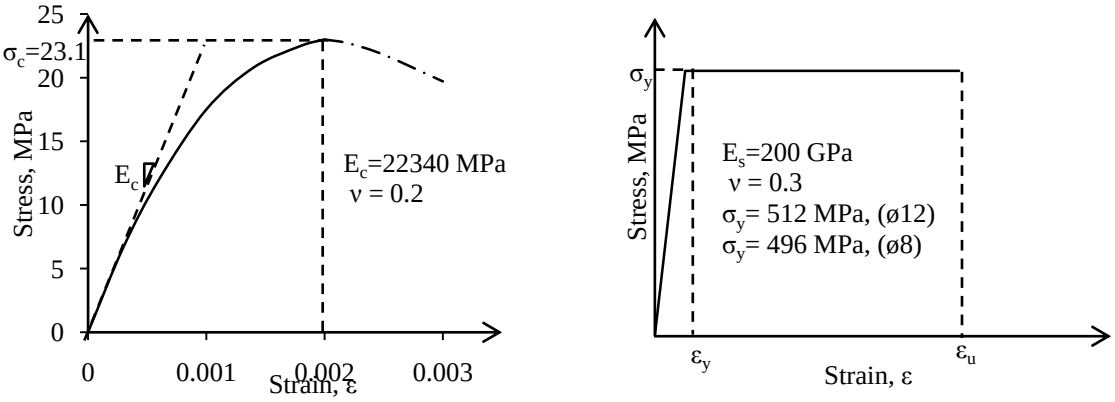

(a) Concrete (b) Reinforcement

Fig. 3 Stress-strain curves for numerical models

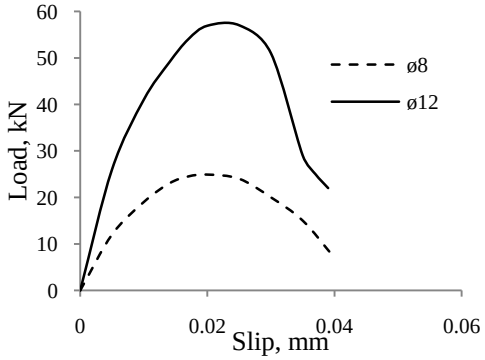

Fig. 4 Load-slip curves of spring elements according to experimental results

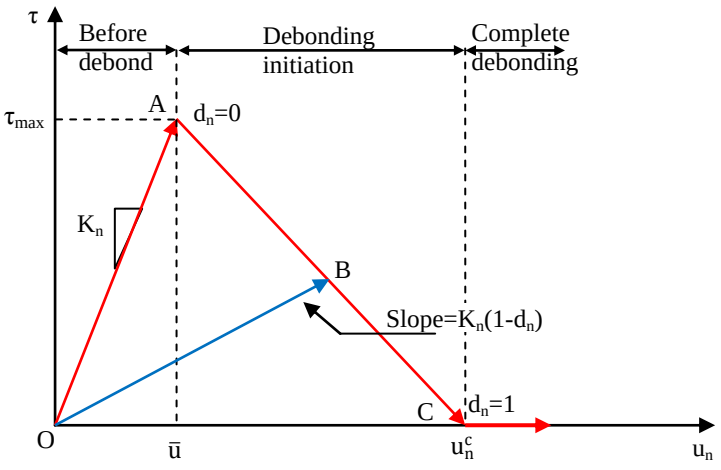

Fig. 5 Bond-slip approach with bilinear CZM

experimental studies, discussed previously, and the average load-slip curves for each of the reinforcements are given in Fig. 4. In the third bond-slip modeling method, the contact surface between the concrete and reinforcement were simulated with Conta174 and Targe170 contact pairs. This method can only be used in models that have three-dimensional reinforcement. In this method, adherence between the reinforcement and surrounding concrete is modeled by combining the bonded contact option with the bilinear cohesive zone material model (CZM) as suggested by Alfano and Crisfield (2001) (Fig. 5) .

This graph can be obtained:

$$\tau = K_n u_n (1-d_n) \tag{5}$$

$$d_n = 0 \quad \text{for} \quad \Delta_n \le 1 \tag{6}$$

$$0 < d_n = \left(\frac{u_n - \bar{u}_n}{u_n}\right)\left(\frac{u_n^c}{u_n^c - \bar{u}_n}\right) < 1 \quad \text{for} \quad \Delta_n > 1 \tag{7}$$

$$\Delta_n = \frac{u_n}{\bar{u}_n} \tag{8}$$

where $\tau, K_n, u_n, \bar{u}_n, u_n^c, d_n$ are bond stress, tangential contact stiffness, slipping distance, slipping distance at the maximum bond stress, slipping distance at the completion of debonding, and debonding parameter, respectively. In this graph, between the OA is a linear elastic area and when maximum bond stress is reached, debonding starts between the connected areas. Linear softening behavior is seen between AC. In this region bond stress decreases gradually and when it reaches point C debonding between the related areas is completed. K_n is the slope of the curve between OA that reflects brittle or ductile debonding. Bilinear CZM curves adopted for experimental results, and to be used in analytical studies, are given in Fig. 6. In Fig. 6, the experimental bond stress of reinforcements were calculated with Eqs. (1)-(2)-(3)-(4) and from the average load-slip curves of the experiments (Fig. 4).

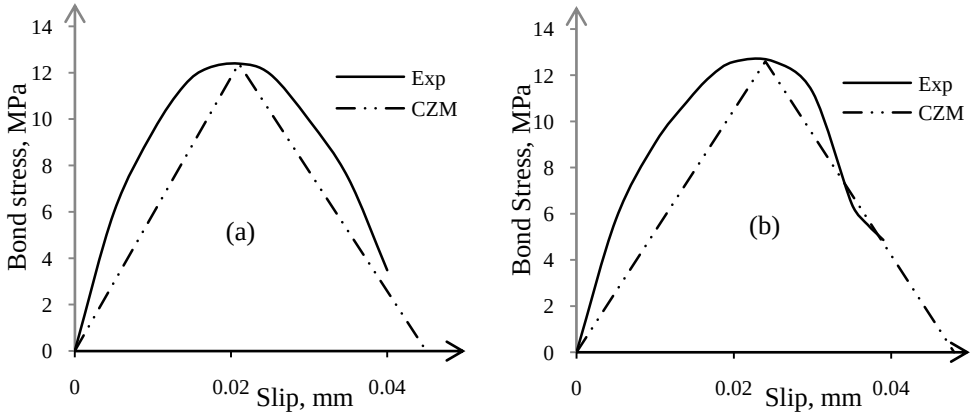

Fig. 6 Bond-slip curves with bilinear CZM, (a) ø8 and (b) ø12

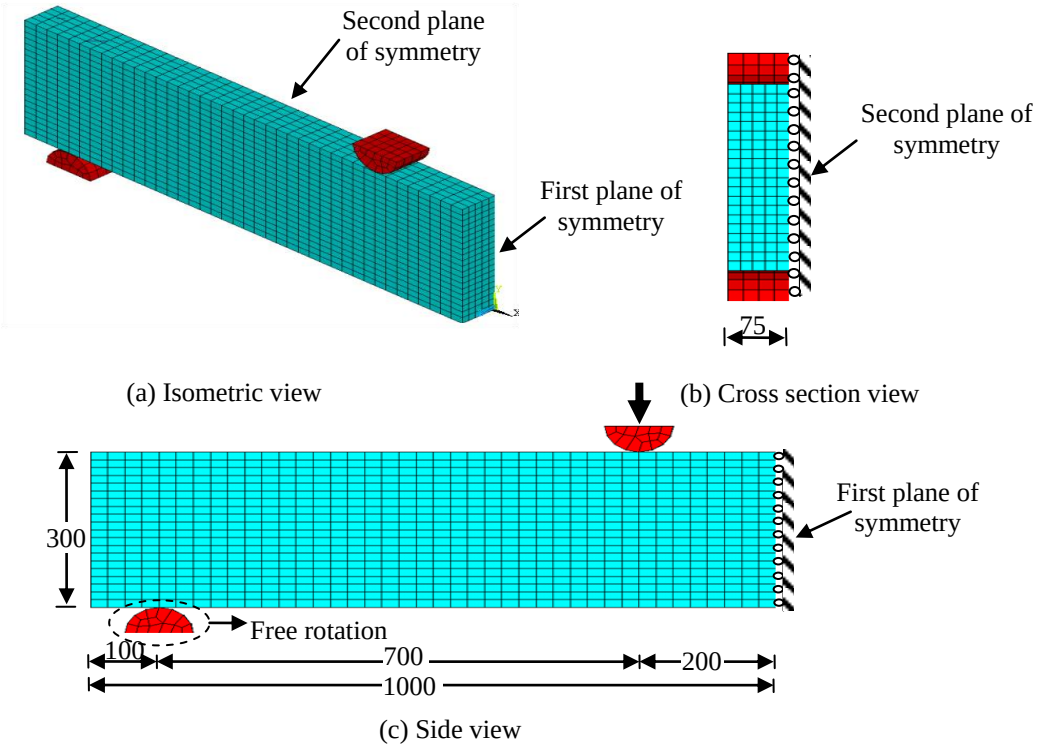

Fig. 7 The developed FE model

Table 4 Properties of FE models

Analysis	Reinforcement		Concrete		Bond-slip	
	Element type	Material model	Element type	Material model	Element type	Material model
LN-PB	Link180	Bkin	Solid65	Miso+Conc	Perfect bond	-
LN-SPR	Link180	Bkin	Solid65	Miso+Conc	Combin39 (Spring)	Multilinear
SLD-PB	Solid45	Bkin	Solid65	Miso+Conc	Perfect bond	-
SLD-CNT	Solid45	Bkin	Solid65	Miso+Conc	Conta174 Targe170	Bilinear CZM
SMRD-PB	-	Bkin	Solid65	Miso+Conc	Perfect bond	-

3.4 Numerical models

Five different numerical models were formed using three different bond-slip modeling methods and three different reinforcement modeling methods, as detailed previously. A quarter of the full

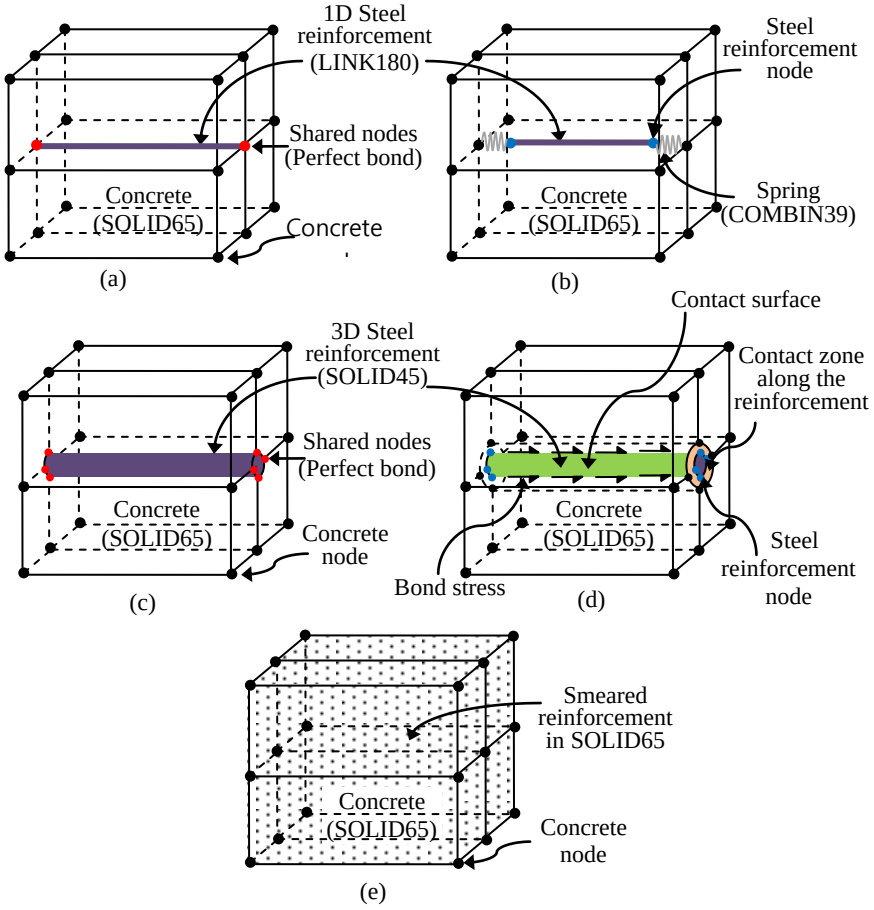

Fig. 8 Reinforcement and bond-slip modeling details of (a) LN-PB, (b)LN-SPR, (c) SLD-PB, (d) SLD-CNT and (e) SMRD-PB

beam was used for finite element modeling by taking the advantage of the symmetry of the beam (Fig. 7). This approach reduced the computation time and computer disk space requirements significantly.

The names and details of created numerical models are given in Table 4. In regards to the naming of numerical models, the first part is represented by the initials of the reinforcement modeling method and the second part by the initials of the bond-slip modeling method. For example, LN-PB indicates that the letters LN denote line elements and PB denotes perfect bond. In the first model named LN-PB, the most common modeling method was used. Reinforcements were modeled with line elements, results showing a perfect bond between the reinforcement and surrounding concrete (Fig. 8(a)). In the second model, named LN-SPR, reinforcements were modeled with line elements and in order to simulate adherence, spring elements were used between the reinforcement and surrounding concrete (Fig. 8(b)).

The first model, in which reinforcements were modeled using three-dimensional solid elements, is SLD-PB (Fig. 8(c)). In this model, perfect bond between the reinforcement and

concrete occurred. In the second model, named SLD-CNT, adherence between the reinforcement and surrounding concrete was achieved with contact elements and also simulated via the CZM model, with bond-slip behavior established according to experimental results (Fig. 8(d)).

The final analytical model employed is SMRD-PB (Fig. 8(e)). In this model, smeared reinforcement was modeled in the concrete with the assumption that perfect bond would occur. In this reinforcement model, reinforcement was not physically modeled; reinforcement exists inside the concrete as volumetric ratio.

Analyses were performed for each of the models and the full Newton-Raphson method was used for the nonlinear analyses. Loads were divided into multiple sub steps until the total load was achieved. Therefore, load deflection curves of beams and strain-deflection curves of longitudinal reinforcements were plotted for comparison with the experimental results.

4. Result and discussion

4.1 Comparison between FEA and experimental results

The load deflection curves of experimentally tested beams are given in Fig. 9. During the test for SP2, some electronic problems occurred in the data collection system and unfortunately results were not available for this specimen. In the comparison of numerical and experimental results, the average curve for SP1, SP3 and SP4 were used (Fig. 10) and results are summarized in Table 5. In the experimental study, the first cracks occured in 2.45, 1.99 and 2.29 mm displacements with 23.51, 26,39 and 27.23 kN load levels for SP1, SP3 and SP4, respectively. The initial stiffness of the curves was calculated as 9.59, 13.26 and 11.9 kN/mm. It was observed that when displacement increased the cracks spread along the beams. At the 10.42, 10.07 and 10.21 mm displacement marks, with 90.31, 94.50 and 96.85 kN loading levels, longitudinal reinforcements yielded under the effects of vertical displacements and bond stress, with crushing evident in the compression zone (Fig. 11). Subsequently, relative displacements between the concrete and the reinforcements started increasing; bond stress capacities being exceeded near the cracks and load-deflection curves appearing as horizontal (Fig. 9). Beams reached maximum loads at 29.57, 27.77 and 27.86

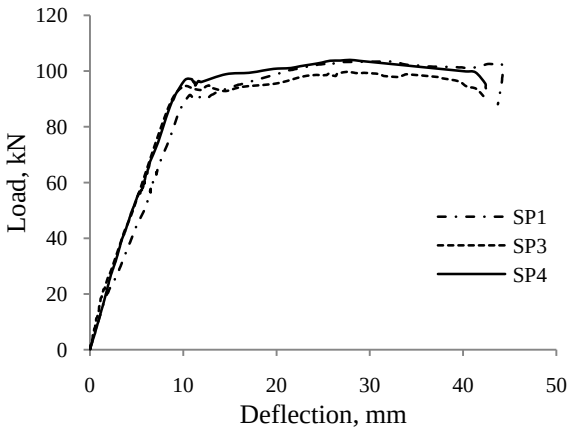

Fig. 9 Experimental results

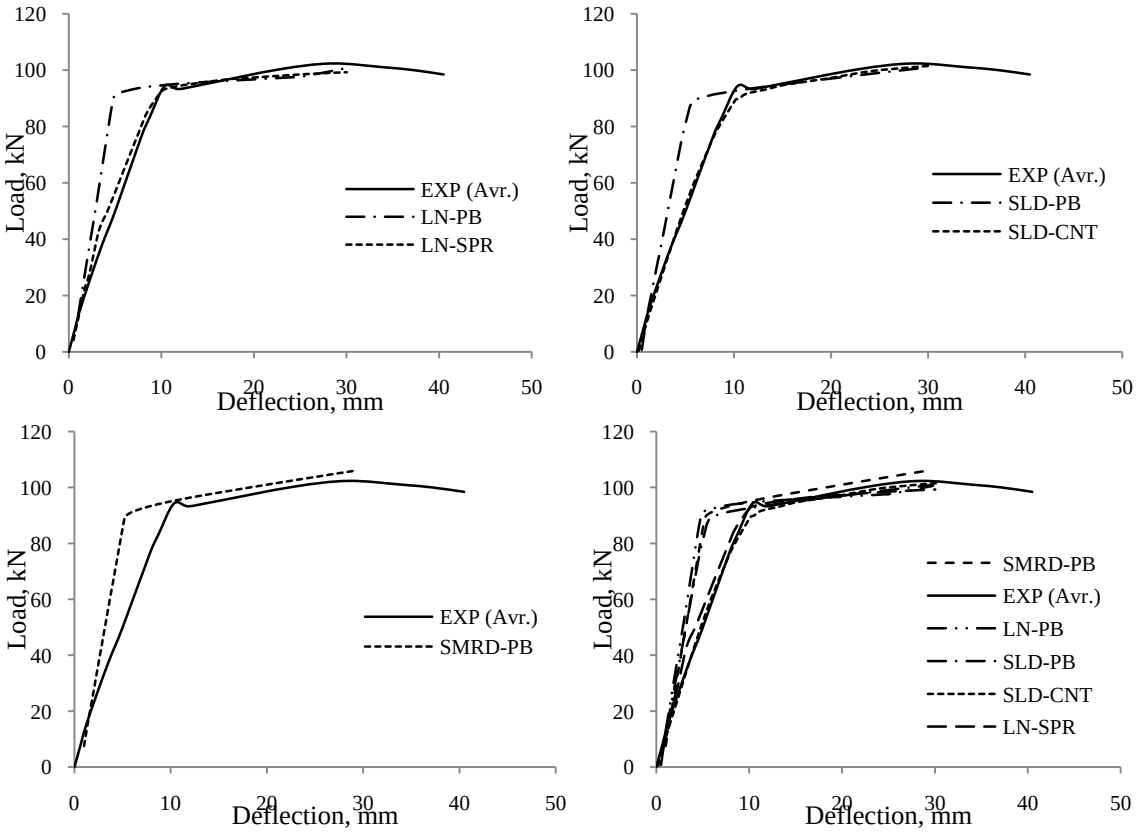

Fig. 10 Comparison of experimental and numerical result

mm displacement with 103.31, 99.80 and 103.98 kN. All test specimens showed similar behavior and failure modes (Fig. 11).

In the numerical studies for LN-PB, SLD-PB and SMRD-PB models, in which perfect bond was considered to have taken place, the initial stiffness was 15.12, 14.01, and 12.82 kN/mm, respectively. In the LN-SPR and SLD-CNT models, which included bond-slip relations, the initial stiffness was 13.17 and 10.58 kN/mm, respectively. As seen in Fig. 10, models having perfect bond have very similar behavior to one another. However, until yielding occurred in the longitudinal reinforcements, the models retained more rigidity according to the experimental results. In the models utilized, including for the bond-slip effect, curves very similar to the average experimental curve were obtained. In the LN-PB, SLD-PB, SMRD-PB, LN-SPR, SLD-CNT models where displacements were 5.13, 5.60, 5.2, 10.05, 10.49 mm and loadings were 91.46, 88, 88.83, 92.53, 89.32 kN respectively, yielding happened in longitudinal reinforcement. These results clearly show that the loading values are very close to the experimental results for all models. In regards to displacements in these loading levels, with perfect bond evident, the percentages, 49.85%, 45.26% and 49.17% respectively, turned out smaller than the experimental results with a ratio of 1.75% and 2.54% for the LN-SPR and SLD-CNT models. After longitudinal reinforcement yielding, all of the numerical models curves exhibited similar behaviors to those of the experimental results. Maximum load values were 100.7, 100.98, 106.07, 99.24 and 101.53 kN

Table 5 Results summary

	Specimens	Yielding Load			Maximum Load		
		P_y (kN)	δ_y (mm)	Error[a] (%)	P_{max} (kN)	δ_{max} (mm)	Error[a] (%)
EXP.	SP1	90.31	10.42	-	103.31	29.57	-
	SP2	n/a	n/a	-	n/a	n/a	-
	SP3	94.50	10.07	-	99.80	27.77	-
	SP4	96.85	10.21	-	103.98	27.86	-
	Avr.[b]	93.89	10.23	-	102.36	28.4	-
FEA	LN-PB	91.46	5.13	49.85	100.60	29.75	4.75
	SLD-PB	88.00	5.60	45.26	100.91	29.80	4.92
	SMRD-PB	88.83	5.20	49.17	106.07	29.31	3.17
	LN-SPR	92.53	10.05	1.75	99.24	30.03	6.70
	SLD-CNT	89.32	10.49	2.54	101.53	30.14	6.13

[a]: % Error of deflections = (1- Avr/FEA)
[b]: Average of experimental results = (SP1+SP3+SP4)/3

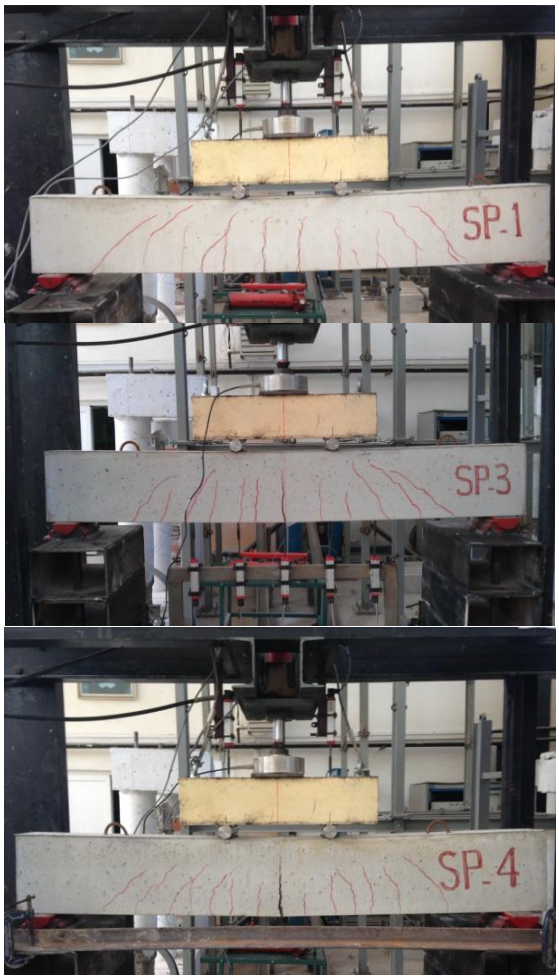

Fig. 11 Failure modes of test specimens

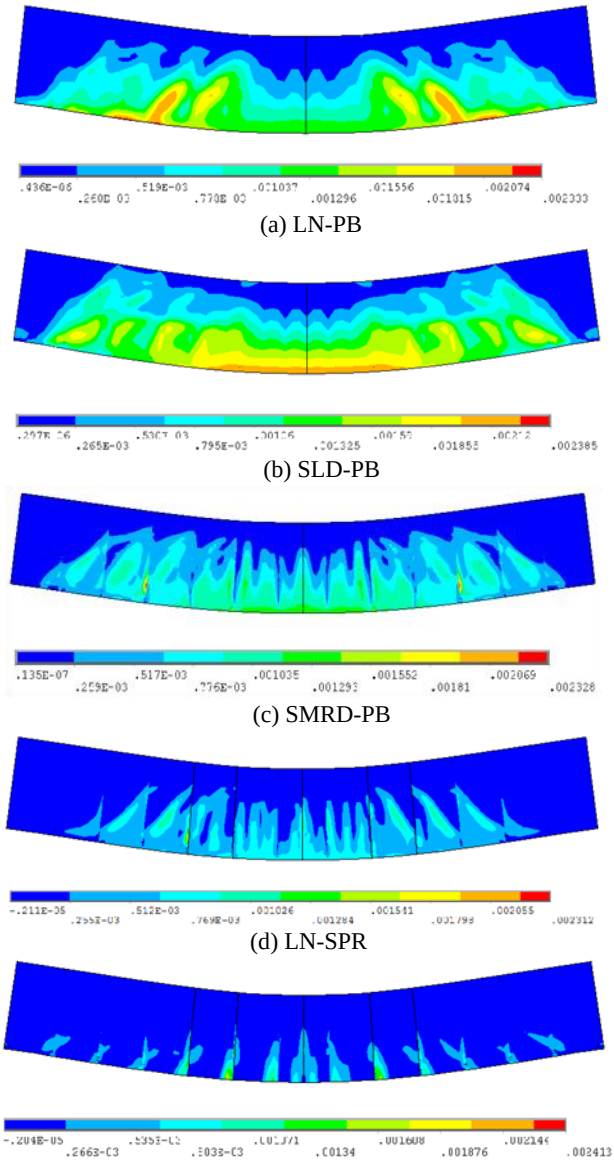

(a) LN-PB

(b) SLD-PB

(c) SMRD-PB

(d) LN-SPR

(e) SLD-CNT

Fig. 12 Bond-slip effect on strain distributions

for LN-PB, SLD-PB, SMRD-PB, LN-SPR and SLD-CNT models and they were 1.62%, 1.35%, 3.62%, 3.05% and 0.81% closer to the experimental results.

In the FE models, strains appearing at the time of longitudinal reinforcement yielding are shown in Fig. 12. In regards to the experimental members, in the regions where concrete tensile strength was exceeded, cracks appeared and adherence between the reinforcement and surrounding concrete disappeared (Fig. 11). Different strains can be seen in these regions' reinforcement and

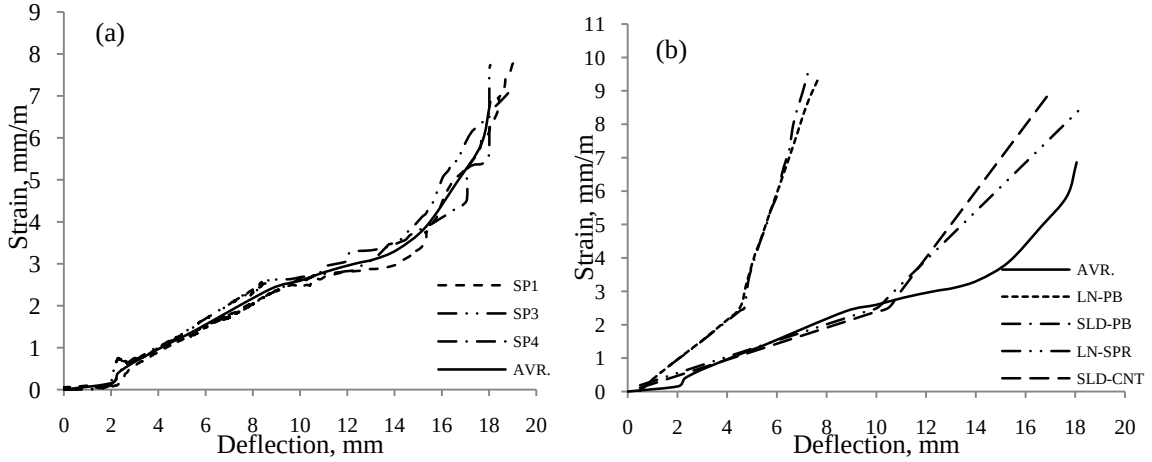

Fig. 13 Strain-deflection curves of longitudinal reinforcement, (a) Experimental results, (b) Comparison of experimental and numerical results

surrounding concrete. In the FE models, considering there was perfect bond, great strains happened when tensile strength in the concrete became too much (Figs. 12(a)-(b)-(c)). Moreover, because of the presence of perfect bond, the reinforcement and surrounding concrete both experienced strains. In regards to the longitudinal reinforcement some unrealistic strains were noted. In Fig. 13(a), strain curves are present in longitudinal reinforcements in the experimental studies. All test specimens showed similar results with each other. Numerical results were compared with the experimental results of the average curve (Fig. 13(b)). According to the average curve for the experimental results, and with longitudinal reinforcement, yielding developed at 9.96 mm. However, in models LN-PB and SLD-PB yielding took place at 5.13 mm and 5.60 mm displacements, respectively. This clearly explains why numerical models reached yielding load at small deflections as well as the reason for the difference between the load-deflection curves (Fig. 10). In the LN-SPR and SLD-CNT models, which included bond slip effects, strains were closer to the experimental results (Fig 12(d)-(e)). In these models, yielding in longitudinal reinforcement resulted at 10.05 mm and 10.49 mm displacements, respectively (Fig. 13(b)). In the SMRD-PB model, it is not possible to produce a strain curve because smeared reinforcement is used.

5. Conclusions

In this study, different bond-slip and reinforcement modeling methods in FE analyses of RC members were investigated with the resulting conclusions compared to the experimental results. In FE analyses, because of the perfect bond occurrence between the reinforcement and surrounding concrete, unrealistic strains occurred in the longitudinal reinforcement after the concrete cracked. This situation greatly affected the load deflection relationship because the longitudinal reinforcements dominated the failure mode. It is highly recommended that the bond-slip relationship is considered in modeling. In addition to the spring elements, the combination of a bonded contact option with CZM also gave closer results to the experimental models. However, modeling of the bond-slip relationship with a contact element was quite difficult and time

consuming. Therefore bond-slip modeling is more suitable with spring elements.

All three methods used for reinforcement modeling gave very close results to each other. In terms of analysis time and ease of modeling one dimensional line elements are more useful. ANSYS accurately predicted the load deflection relationships up to the point when compressive crushing became dominant.

References

Alavi-Fard, M. and Marzouk, H. (2002), "Bond behavior of high strength concrete under reversed pull-out cyclic loading", *Can. J. Civ. Eng.*, **29**(2), 191-200.

Alfano, G. and Crisfield, M.A. (2001), "Finite element interface models for the delamination anaylsis of laminated composites: mechanical and computational issues", *Int. J. Numer. Meth. Eng.*, **50**, 1701-36.

Altun, F. and Birdal, B. (2012), "'Numerical investigation of a three-dimensional FRP-retrofitted reinforced concrete structure's behaviour under earthquake load effect in ANSYS program", *Nat. Hazard. Earth. Syst. Sci.*, **12**, 3701-3707.

ANSYS (2014), Academic Research, Release 15.0.

Arslan, M.E. and Durmuş, A. (2014), "Fuzzy logic approach for estimating bond behavior of lightweight concrete", *Comput. Concrete*, **14**(3), 233-245.

Ashtiani, M.S., Dhakal, R.P., Scott, A.N. and Bull, D.K. (2013), "Cyclic beam bending test for assessment of bond-slip behavior", *Eng. Struct.*, **56**, 1684-97.

Aslani, F. and Samali, B. (2013), "Predicting the bond between concrete and reinforcing steel at elevated temperatures", *Struct. Eng. Mech.*, **48**(5), 643-660.

Barbosa, A.F. and Ribeiro, G.O. (1998), "Analysis of reinforced concrete structures using ANSYS nonlinear concrete model", *Comput. Mech., New Trend. Appl.*, 1-7.

Campione, G., Cucchiara, C., La Mendola, L. and Papia, A. (2005), "Steel-concrete bond in lightweight fiber reinforced concrete under monotonic and cyclic actions", *Eng. Struct.*, **27**(6), 881-90.

Cattaneo, S. and Rosati, G. (2009), "Bond between steel and self-consolidating concrete: experiments and modeling", *ACI Struct. J.*, **106**(4), 540-50.

Chen, G.M., Chen, J.F. and Teng, J.G. (2012), "On the finite element modelling of RC beams shear strengthened with FRP", *Constr. Build. Mater*., **32**, 13-26.

De Almeida Filho, F.M., El Debs, M.K. and El Debs, A.L.H.C. (2008), "Bond-slip behavior of self-compacting concrete and vibrated concrete using pull-out and beam tests", *Mater. Struct. Mater. Constr.*, **41**(6), 1073-89.

Demir, S., Husem, M. and Pul, S. (2014), "Failure analysis of steel column-rc base connections under lateral cyclic loading", *Struct. Eng. Mech.*, **50**(4), 459-469.

Desnerck, P., De Schutter, G. and Taerwe, L. (2010), "Bond behavior of reinforcing bars in self-compacting concrete: experimental determination by using beam tests", *Mater. Struct. Mater. Constr*., **43**, 53-62.

Eligehausen, R., Popov, E. and Bertero, V. (1983), "Local bond stress-slip relationships of deformed bars under generalized excitations", Report No. UCB/EERC-83/23, Earthquake Engineering Research Center, University of California, Berkeley

Ersoy, U. (2012), *Reinforced Concrete*, Metu Press, Turkey.

Fang, C.Q., Gylltoft, K., Lundgren, K. and Plos, M. (2006), "Effect of corrosion on bond in reinforced concrete under cyclic loading", *Cement Concrete Res.*, **36**(3), 548-55.

Fallah, M.M., Shooshtari, A. and Ronagh, H.R. (2013), "Investigating the effect of bond slip on the seismic response of RC structures", *Struct. Eng. Mech.*, **46**(5), 695-711.

Hawileh, R.A. (2012), "Nonlinear finite element modeling of RC beams strengthened with NSM FRP rods", *Constr. Build. Mater*., **27**, 461-71.

Kachlakev, D. and Miller, T. (2001), "Finite element modelling of reinforced concrete structures stregthened with FRP laminates", Final Report, SPR 316, Oregon Department of Transportation Research Group and

Federal Highway Administration.
Kamal, M.M., Safan, M.A. and Al-Gazzar, M.A. (2013), "Steel-concrete bond potentials in self-compacting concrete mixes incorporating dolomite powder", *Adv. Concrete Constr.*, **1**(4), 273-288.
Kwan, W.P. and Billington, S.L. (2001), "Simulation of structural concrete under cyclic loading", *J. Struct. Eng.*, **127**(12), 1391-1401.
Livaoglu, R. and Durmus, A. (2015), "Investigation of wall flexibility effects on seismic behavior of cylindrical silos", *Struct. Eng. Mech.*, **53**(1), 159-172.
Marzec, I., Skarżyńskia, L., Bobińskib, J. and Tejchmanc, J. (2013), "Modelling reinforced concrete beams under mixed shear-tension failure with different continuous FE approaches", *Comput. Concrete*, **12**(5), 585-612.
Mirza, S.M. and Houde, J. (1979), "Study of bond stress-slip relationships in reinforced concrete", *ACI J. Pr.*, **76**(1), 19-46.
Nielsen, M.P. (1998), *Limit Analysis and Concrete Plasticity*, CRC Press, USA.
RILEM-FIP-CEB. (1973), "Tentative recommendations, recommendations for reinforcing steel, bond test for reinforcing steel: 1-beam test (7-ii-28 d) 2-pull-out test (7-ii-128)", *Mater. Struct.*, **6**(2), 79-118.
Padmarajaiah. S.K. and Ramaswamy, A. (2002), "A finite element assessment of flexural strength of prestressed concrete beams with fiber reinforcement", *Cement Concrete Compos.*, **24**, 229-41.
Tepfers, R. (1973), *A theory of Bond Applied to Overlapped Tensile Reinforcement Splices for Deformed Bars*, Chalmers University of Technology, Goteborg.
Wei-ping, Z. (2011), "Local bond-slip numerical simulation based on ANSYS contact analysis", *Proceedings of the 3rd International Conference on Computer Engineering and Technology*, Kuala Lumpur, June.
Willam, K.J. and Warnke, E.P. (1974), "Constitutive model for the triaxial behaviour of concrete", *IABSE*, Report No.19, Bergamo, 1-30.
Wolanski, A.J. (2004), "Flexural behaviour of reinforced and prestressed concrete beams using finite element analysis", Degree of Master of Science,Marquette University, Wisconsin.
Xiaroran, L.I. and Yuanfeng, W. (2010), "Three-dimensional nonlinear finite element analysis of reinforced concrete structures based on ANSYS program", *Proceedings of the 2nd International Conference on Computer Engineering and Technology*, Chengdu, April.
Yang, Z.J. and Chen, J. (2005), "Finite element modelling of multiple cohesive discrete crack propagation in reinforced concrete beams", *Eng. Fract. Mech.*, **72**, 2280-97.
Zhao, J. and Sritharantharan, S. (2007), "Modeling of strain penetration in fiber based analysis of reinforced concrete structures", *ACI Struct. J.*, **104**(2), 134-14.

CC